RSC Advances




ROYAL SOCIETY OF CHEMISTRY

www.rsc.org/advances

# Development of a multiple reaction monitoring (MRM) method based on high performance liquid chromatography/tandem mass spectrometry to analyze *in vivo* exposure profiles of complex herbal components independent of standards

T. Xie[1], A. Kang[2], J. Xu[1], C. Shen[1], X. Zhao[1], L. Di[2], S. Wang[1], J. Shan[1,2*]

*1. Jiangsu Key Laboratory of Pediatric Respiratory Disease, Institute of Pediatrics, Nanjing University of Chinese Medicine, Nanjing 210023, China*

*2. Jiangsu Engineering Research Center for Efficient Delivery System of TCM, College of Pharmacy, Nanjing University of Chinese Medicine, Nanjing 210023, China*

[*] Corresponding author, Tel.:+86 85811330; E-mail Address: jshan@njutcm.edu.cn

**Abstract**

Exposure profiles of herbal components *in vivo* play pivotal roles in pharmacodynamic evaluation. Herein, we report the development of a universal multiple reaction monitoring (MRM) method for the sensitive and accurate identification of *in vivo* exposure profiles of complex herbal systems, including exposure components, exposure times, and relative exposure levels. The method integrated multiple scan monitoring types based on high performance liquid chromatography/tandem mass spectrometry (HPLC/MS-MS), and mainly consisted of four steps: (a) analyzing herbal extract samples by high resolution mass spectrometry, (b) refining S-lens and CE voltages to develop the MRM method, (c) detecting exposure components, and (d) evaluating exposure times and levels. We applied this developed method step-by-step to delineate the flavonoid profiles of *Schisandra chinensis* extract, detecting 22 exposure flavonoids of which 19 were defined as long-term exposure components. Using a "relative exposure approach," relative exposure levels *in vivo* were further elucidated. Compared with the general method based on high resolution MS-based HPLC/linear trap quadrupole (LTQ)-Orbitrap, the improved method provided more comprehensive detection. Furthermore, we demonstrated the utility of this approach in the investigation of exposure profiles of pyridine alkaloids in *Tripterygium wilfordii Hook.F.* extract. Of 55 MRM transitions, 39 exposure components were detected. The results of this study suggested that the improved method might provide an excellent foundation for sufficient, sensitive, and accurate monitoring of exposure profiles in complex herbal systems

or homologous compounds *in vivo*.

**Keywords:** Exposure profiles, herbal systems, *Schisandra chinensis* extract, *Tripterygium wilfordii Hook.F.* extract, HPLC/MS-MS

## Introduction

Many people, particularly in East and Southeast Asia, believe herbs to be preventive medicines and cures for various chronic ailments. A great number of herbs have been administered as oral medication. However, their efficacy is still questioned, in part due to insufficient knowledge about their exposure profiles *in vivo*. In this regard, exposure in systemic circulation is believed to be most important for exerting efficacy, with much literature concerning perspectives on exposure components[1]. Exposure time and level also exert effects on pharmacodynamics. For example, the mechanistic pharmacodynamic model can accurately predict drug efficacy by considering drug residence time[2-4]. Such findings further demonstrated that depicting and elucidating exposure profiles of complex herbal systems *in vivo* play significant roles in evaluating efficacy, drug safety, disposition, and metabolic behavior, providing valuable information for dissecting the effective mechanism and assessing treatment response.

Herbs are complex systems containing many homologous components. It is now common to focus on the detection of exposure components and metabolites *in vivo* in

order to understand the fundamental role of exposure profiles in physiological functions[5-7]. In exposure profiling, especially by oral administration, the analytical response, herb content, and bioavailability all affected exposure profiles. In particular, the development of high resolution mass spectrometry enabled accurate analysis of herbal exposure components in dosed rat plasma, including flavones[8, 9], alkaloids[10], and saponins[11, 12], due to its advantages in specificity and structural characterization. Based on accurate mass measurement and $MS^n$ fragmentation, much progress was achieved. In fact, these studies characterized multiple exposure components and previously unreported metabolites. However, the detection of absorbed components was always restricted to one or two designated time points after administration, potentially resulting in the omission of components with short exposure times. Currently, exposure components are not routinely evaluated. Exposure times and levels should be further taken into consideration. Recently, Liang *et al.* developed a sensitive HPLC/ion trap (IT)-time of flight (TOF) MS method to profile the pharmacokinetic behavior of lignans in *Schisandra chinensis*, independent of standards, while proposing a relative exposure approach to describe exposure levels[13]. However, limited dynamic ranges and high limits of detection (LODs) restrict their application in the quantitative analysis of a wider range of components. Instead, a multiple reaction monitoring (MRM) method based on a triple quadrupole mass spectrometer was preferred for quantitative analysis, whether *in vivo* or *in vitro*, exogenously[14] or endogenously[15]. Li *et al.* reported an effective derivative multiple reaction monitoring (DeMRM) method for direct and rapid transition development, which semi-quantified a total of 138 components in herbs or decoctions. However, the method was not applied to *in vivo* analysis[16].

To address the above problems, we sought to develop a modified HPLC/MS-MS-based MRM method that could profile exposure components sensitively, robustly, and universally. Due to the inaccessibility of standards, it was necessary to properly tune the mass parameters to achieve optimal analytical performance. Using this modified approach, we successfully elucidated the exposure profile *in vivo* of *Scutellaria baicalensis* extract. Furthermore, another herb, *Tripterygium wilfordii Hook.F.*, was analyzed to validate the method, showing that the technique was able to accurately screen exposure components and successfully characterize the exposure time and levels. We believe that our improved method is tailored to herbal medicines, and is expected to be generally applicable across all complex herbal systems.

## Experimental

**Materials and chemicals**

*Scutellaria baicalensis* tubers (batch number, 20131219) were purchased from the Anhui Fengyuan Tongling Chinese Herbal Medicine Co., Ltd. (Anhui, China), and *Tripterygium wilfordii Hook.F.* (batch number, 20150620) was purchased from the Jiangsu Meitong Pharmaceutical Co., Ltd. (Jiangsu, China). The two herbs were both authenticated according to their morphological characteristics by Liu Shengjin PhD., Nanjing University of Chinese Medicine. Standards of liquiritigenin, kaempferol, quercetin, chrysin, apigenin, baicalin, wogonin, oroxylin A, isorhamnetin, baicalein, scutellarin, wogonoside, oroxin A, oroxin B, luteolin-7-glucoside, and wilforine were purchased from the National Institute for the Control of Pharmaceutical and Biological Products (Beijing China). The purity of all standards was >99%. All aqueous solutions were prepared with deionized water purified by a Milli-Q Ultrapure water system (Millipore, Bedford, USA). HPLC-grade acetonitrile and methanol were purchased from Fisher Scientific (Fair Lawn, NJ, USA). Other chemicals and solvents were all of analytical grade.

**Herbal and plasma preparation**

*Scutellaria baicalensis* tubers (50 g) were extracted with 70% ethanol (500 mL) under reflux for 2 h then filtered. A further 400 mL 70% ethanol was subsequently added to the residues, which were refluxed for another 2 h. After that, the two extracts were mixed, filtered, and evaporated to dryness under reduced pressure. The resultant residue was dissolved in water (50 mL) and vortexed for 10 min. After centrifugation at 20,000 rpm for 10 min, the supernatant was transferred into tubes for qualitative analysis and animal study.

*Tripterygium wilfordii Hook.F.* tubers (60 g) were twice extracted with water (600 mL) in an electromagnetic oven. The two extracts were then mixed, filtered, and evaporated to dryness under reduced pressure. The residue was dissolved in 50 mL water. After centrifugation at 20,000 rpm for 10 min, the supernatant was transferred into tubes for qualitative analysis and animal study.

Plasma samples were prepared by methanol precipitation. Aliquots of 30 μL plasma sample and 10 μL internal standard (2 μg/mL liquiritigenin for *Scutellaria baicalensis* extract, 0.5 μg/mL wogonin for *Tripterygium wilfordii Hook.F.* extract) were extracted using 100 μL ice cold methanol. After vigorous vortexing for 10 min, the

sample tube was centrifuged at 18,000 g for 5 min. An 80 μL aliquot was transferred to a vial and 2 μL was injected for analysis by HPLC/MS-MS. As the concentrations of analytes in the plasma samples exceeded the linearity range, the samples were diluted appropriately with blank plasma.

**Chromatogram separation and mass spectrometry conditions**

For the detection of flavonoids in *Scutellaria baicalensis* extract, qualitative data was acquired by an LTQ-Orbitrap mass spectrometer (Thermo Fisher Scientific, San Jose, CA) coupled with an HPLC model U3000 apparatus (Dionex, San Jose, CA). Instrument control, data acquisition, and analysis were performed using Thermo Xcalibur 2.2 SP1.48. Chromatographic separation was achieved on a Thermo BDS Hypersil $C_{18}$ (2.1 mm × 100 mm, 2.3 μm) column with the column temperature set at 40 °C. The mobile phase consisted of solvent A; 0.1% formic acid in water, and solvent B; 0.1% formic acid in acetonitrile. The mobile phases were eluted at 0.25 mL/min. The gradient was as follows: 10% B for 3.0 min, increased to 50% at 40 min, increased further to 80% at 42 min, and then decreased to 10% at 44 min, followed by 5 min equilibration. The LTQ-Orbitrap mass spectrometer was operated with the following parameters: spray voltage, 3.5 kV; heated capillary, 300 °C; HESI probe, 350 °C; sheath gas pressure, 40 psi; auxiliary gas pressure, 15 psi. These conditions were kept constant for both positive and negative ionization mode acquisition. The mass calibration was corrected using the standard calibration mixture before analysis. Accurate mass was used to predict the formula (ppm < 5). For full mass scan analysis, spectra were recorded in the range of *m/z* 200–800. $MS^n$ data were triggered by the data-dependent acquisition mode. Target ions were selected for fragmentation by dynamic exclusion for 10 s. The normalized collision energy for $MS^2$, $MS^3$, and $MS^4$ was 35, and the ion selection threshold was 10000, 1000, and 500 counts, respectively.

The detection of exposure components and pharmacokinetic data was achieved using a Thermo TSQ Vantage tandem mass spectrometer (Thermo Fisher Scientific, San Jose, CA) coupled with an HPLC model U3000 apparatus (Dionex, San Jose, CA). The mass spectrometer was interfaced with an HESI source. For the detection of *Scutellaria baicalensis* extract, the mobile phase and conditions for the chromatographic column were identical to those of the HPLC/LTQ-Orbitrap-MS. To shorten the analysis cycle, elution was optimized as follows: 25% B maintained for 1.0 min, increased to 60% at 5.5 min, increased to 75% at 12.5 min, and then decreased to 25% at 15 min. The ion source parameters were identical to those described above for the LTQ-Orbitrap-MS. The scan time is 0.04s for detection for flavonoids and pyridine alkaloids.

For the detection of *Tripterygium wilfordii Hook.F.*, the mobile phase consisted of solvent A; 0.1% formic acid in water, and solvent B; 0.1% formic acid in methanol. The flow was 0.25 mL/min. The separation gradient was as follows: 35% B maintained for 1.0 min, increased to 90% at 7 min, maintained for 2 min, and then decreased to 35% at 11 min, followed by 4 min equilibration. The HPLC/LTQ-Orbitrap-MS spectra were recorded in the range *m/z* 200–1000. Other chromatogram column separation conditions and the mass spectrometry ion source were the same as for *Scutellaria baicalensis* extract.

**Animal study**

Sprague-Dawley rats (male, weighing 200 ± 20 g) were obtained from Shanghai Jie Sijie experimental animal Co., Ltd. (Shanghai, China) and kept in an environmentally controlled breeding room for at least 7 days before experimentation. The rats were fasted overnight but with free access to water before the tests. Animal welfare and experimental procedures were strictly in accordance with the guide for the care and use of laboratory animals. Six rats were intragastrically administered a 10 g/kg crude single dose of *Scutellaria baicalensis* extract. Approximately 80 μL heparinized blood samples were collected at 0.08, 0.17, 0.25, 050, 0.75, 1.0, 2.0, 4.0, 6.0, 8.0, 10.0, 12.0, 15.0, 24.0, and 30.0 h from the ophthalmic veins and immediately centrifuged at 4000 g for 5 min to obtain the plasma. Another six rats were intragastrically given 12 g/kg crude *Tripterygium wilfordii Hook.F.* extract. Blood samples were collected at 0.08, 0.17, 0.33, 050, 0.75, 1.0, 2.0, 4.0, 6.0, 8.0, 10.0, 12.0, and 24.0 h to obtain the plasma. All of the plasma samples were stored at -20 °C until analysis. All the animal experiments were approved by institutional committee of Nanjing University of Chinese Medicine and conducted in compliance with the guidelines for animal handing.

**Pharmacokinetic analysis of *Scutellaria baicalensis* extract**

The herbal pharmacokinetics of *Scutellaria baicalensis* extract were assessed by a "relative exposure approach" reported by Liang *et al.* [13]. The plasma concentration was expressed as the relative concentration, as estimated for crude herbal extracts, by preparing "mixed calibration curves." Briefly, the *Scutellaria baicalensis* extracts were sequentially diluted by twice their mass of methanol to give working solutions. The working solutions (3 μL) were then spiked into blank rat plasma (30 μL) to prepare the

"mixed calibration curves," accounting for relative concentrations of 0.01–10 mg/mL for the crude materials. After that, the relative concentration was identified as the independent variable, and the mass-response ratio of targeted analytes to internal standards was the dependent variable for linear regression. The accuracy and precision of the method were established by analyzing quality control (QC) samples of 0.01953, 0.1563, and 1.25 mg/mL *Scutellaria baicalensis* extract in 3 analytical runs, accompanied by a set of calibration samples in each run. The accuracy was determined as the percentage difference between the mean and expected concentrations. The coefficient of variation measured intra- and inter-day precision.

Pharmacokinetic parameters were calculated by DAS 2.0 software package (BioGuider Co., Shanghai). Due to the bimodal distribution of flavonoids, we applied a non-compartmental pharmacokinetic model to obtain parameters.

## Results and discussion

In the present study, complete processing of the modified MRM method was achieved by HPLC/MS-MS, and consisted of the following four steps: (a) analyzing herbal extract samples by high resolution mass spectrometry to collect MS/MS fragmentation spectra and provide tentative identification; (b) screening detectable precursors and optimizing S-lens and CE values for developing a MRM method for quantification of the components; (c) using the developed MRM method to analyze all dosed plasma samples at different points to detect exposure components; and (d) determining exposure times and levels.

### Qualitative analysis of *Scutellaria baicalensis* extract by HPLC/LTQ-Orbitrap-MS

Before the analysis of exposure components, herbal-sourced chemical flavonoids were characterized by HPLC/LTQ-Orbitrap-MS. The obtained chemicalome profiling results can ensure the accuracy of subsequent characterizations of exposure flavonoids. Both positive and negative ionization modes were conducted for total flavonoid coverage. Fig. 1A and 1B show the representative positive and negative total ion chromatograms (TICs) of the flavonoid constituents in *Scutellaria baicalensis* extract, with 143 flavonoids detected in total. To facilitate analysis for structural characterization, flavonoids were divided into five types based on their fragmentation: I, flavonoid

aglycones without methoxy groups; II, methoxylated flavonoid aglycones; III, *O*-glycosyl flavonoids; IV, *C*-glycosyl flavonoids; and V, flavonoid sulfates. The results indicated that most *C*-glycosyl flavonoids and flavonoid sulfates were eluted at 3-15 min, the *O*-glycosyl flavonoids were eluted at 13-23 min, and the flavonoid aglycones and methoxylated flavonoid aglycones were eluted at 20-35 min. Using diagnostic ion and neutral loss analyses, the structures of 133 compounds were successfully characterized. Ten peaks failed to match a reasonable structure due to ambiguous $MS^n$ information. The structures of the identified compounds are shown in Fig. 2. Detailed positive and negative fragment information is illustrated in supplementary information Table S1. The fragmentation of flavonoids with different structures has been detailed numerous times in the literature and we have given a brief summary below[17, 18].

For flavonoid aglycones, fragments at $[M+H–H_2O]^+$, $[M+H–CO]^+$, $^{1,3}A^+$, $^{1,3}B^+$, $^{0,2}B^+$, $^{0,4}B^+$, and $^{0,4}B^+–H_2O$ were prevalent in the positive $MS^2$ spectra, while $[M–H]^-$ ions of the flavonoid aglycones gave rise to predominant fragment ions at $[M–H–H_2O]^-$, $[M–H–CO]^-$, $[M–H–CO_2]^-$, $[M–H–CO–CO_2]^-$, $[M–C_2H_2O]^-$, $^{1,3}A^-$, and $^{1,3}B^{-}$[19]. In general, the $^{1,3}A^+$ and $^{1,3}A^-$ ions, always observed as strong peaks, served as the diagnostic products for flavonoid aglycones. Twenty-one flavonoid aglycones were detected by diagnostic analysis, with 20 structurally characterized.

Methoxylated flavonoids were easily detected by the loss of 15 mass units from precursor ions. This uncommon transition from an even-electron to an odd-electron ion was found to be unique for methoxylated flavonoids. Except for the characteristic $[M+H–CH_3\cdot]^{+\bullet}$ and $[M–H–CH_3\cdot]^{-\bullet}$ ions, fragmentation was similar to that of the non-methoxylated flavonoids[20]. Using this characteristic mass loss, 36 methoxylated flavonoids were detected.

Glycosidic bond cleavage during *O*-glycosylation producing predominant aglycone ions in the $MS^2$ spectra was the characteristic fragmentation for *O*-glycosyl flavonoids. The detailed structure of the aglycone moiety was further deduced from the $MS^3$ or $MS^4$ spectra in comparison with the $MS^2$ spectrum of related aglycone flavonoids. In total, 49 compounds were detected of which 15 were mono-glucosyl flavonoids, 20 were mono-*O*-glucuronosyl flavonoids, and 3 were di-glucosyl flavonoids. Additionally, 8 glucuronosyl methyl ester conjugates were characterized from fragments with a neutral loss of 190 mass units.

Instead of generating abundant aglycone ions, as for *O*-glycosides, the $MS^2$ spectra of *C*-glycosides showed successive elimination of two or three $H_2O$ molecules[21-23]. Vukics *et al.* have summarized characteristic mass losses for glycosyl cleavage, which were particularly useful for structural characterization[17]. In accordance with these

characteristic fragments, 21 compounds were detected, with structures identified for 19: 2 mono-*C*-glycosyl flavonoids, 11 di-*C*-glycosyl flavonoids, 1 *O*-glycosyl-*C*-glycosylflavonoid, 4 *C*-glycosyl flavanones, and 1 *C*-glycosyl dihydrochalcone.

Flavonoid sulfates were also isolated in our study, since sulfur fumigation was always carried out for dyeing, insecticide, and whitening effects. These flavonoid sulfates preferentially produced a neutral mass loss of 80 units, corresponding to the loss of $SO_3$ in negative ionization mode[24]. In total, 15 sulfated flavonoids were determined, 12 of which were identified according to their $MS^3$ and $MS^4$ spectra.

**Development of the modified MRM method for the quantification of herbal components**

Full mass scans were next used to select detectable precursors of the herbal samples. We considered that quantitative analysis of exposure compounds usually contained lots of samples to be analyzed (usually >150 samples, and more than 5 day to analysis if 45 min eluted time was used). Relative long elution time will affect the stability and repeatability. Base on the above consideration, we re-optimized eluted time, although the isomer compounds will co-eluted. Since the relative few compounds of *C*-glycosyl flavonoids and flavonoid sulfates were detected at the high water phase elution time, we started phase B from 25% to short the elution time. However, in order to give the sufficient separation of the wogonin and oroxylin A, wogonoside and oroxin A (high content in *Schisandra chinensis* extract and obvious pharmacological effect), the gradient was slowed down from the 60-75 % phase B in 6 min. Finally, the eluted gradient controlled within 15min (Fig. 1C). For potential identification, the matching degree of the $MS^2$ spectra and elution order were used to match the peaks produced from the LTQ-Orbitrap-MS. A total of 22 peaks were finally screened out. Interestingly, most of the HPLC/MS-MS peaks showed corresponding assignments in the HPLC/LTQ-Orbitrap-MS spectra, since it produced similar $MS^2$ spectra to that of LTQ. For example, HPLC/MS-MS peak *m/z* 549.2 eluting at 1.77 min, gave a similar $MS^2$ spectrum to that of peak 13 from the LTQ-Orbitrap-MS, as illustrated in Fig. 3B and Fig. 3C, showing a small difference in the relative abundance of products. However, the isomer eluting at 1.96 min gave different $MS^2$ spectra between the MS/MS and LTQ fragmentation. MS/MS produced abundant products, and gave a base peak at *m/z* 363.2 as the CE value increased. These products may be produced from $[M–150–18+H]^+$, but no similar $MS^2$ spectrum was observed in LTQ fragmentation. In fact, according to elution order, we empirically assigned it to LTQ-Orbitrap-MS peak 22, which

produced primary products at $[M–18+H]^+$, $[M–36+H]^+$ and $[M–54+H]^+$ (supplementary information Fig S1A and S1B). The obviously different fragmentation between MS/MS and LTQ suggests that, even though the position isomers, the parameter settings should be adjusted and optimized so that they are more explicit and unbiased for MRM detection. For the matching of other peaks, it can be referred to Tables 1 and S1.

A similar case was observed for the elution order. Most components showed identical elution order in HPLC/MS-MS and HPLC/LTQ-Orbitrap-MS, except for oroxylin A. Four different elution conditions were used to compare the eluted order of the oroxylin A (peak 139) in HPLC/LTQ-Orbitrap-MS. An interesting results were observed. As the shorter of the eluted time, the eluted order of the three peaks changed, and oroxylin A eluted after the peak 140 and peak 142 which was consistent with that of LC-MS-MS separation system (Supplementary information Fig. S2). Actually, some literatures reported that the eluted order was reversed by changing the mobile phase conditions[25, 26]. Thus, it should be careful and step by step to re-optimized the elution gradient.

After precursor detecting, CEs and S-lens were refined. Of the 22 potential exposure components, compounds accessible as standards were optimized under direct infusion of the single compounds. Others proved more challenging because of the absence of standards. Parameters of CEs and S-lens were found to be very important for the detection sensitivity. Between the two, S-lens was regarded as a compound-dependent parameter. In this study, we employed selected ion monitoring with different S-lens to optimize this parameter during chromatographic separation. Fig. 4 shows the two peaks detected at *m/z* 549.2. The results indicated that the highest area was observed using 100 V S-lens for earlier eluted peaks, and 90 V for the later eluted peaks. Next, under the same chromatographic separation conditions similarly, we performed product ion monitoring at different collision energies to select the most stable products and CE values with the highest response. The collision energy range was set at 18–30 eV with reference to the optimized parameters of the standards. In order to obtain unbiased product information, the scan event was monitored to ensure at least 2 scan points for each peak. Fig. 3A shows the $MS^2$ TICs of the products from *m/z* peak 549.2 by product ion monitoring. Obviously, the two isomerism peaks were profiled, corresponding to the TICs from selected ion monitoring, although each peak was collected at 3 scan points. Fig. 3C–J demonstrate the product spectra at $t_R$ 1.78 min. Notably, MS/MS produced similar $MS^2$ spectra to those of LTQ-Orbitrap-MS, with only small differences in fragment abundance. The results of different CEs indicated that a CE of 18 eV produced a stable, highest intensity product at *m/z* 411.2. Combined with S-lens optimization, peak *m/z* 549.2 at 1.78 min yielded MRM transition 549.2 →

411.1 (S-lens and CE set at 100 V and 18 eV, respectively). Other peaks were optimized using the same procedure. It should be mentioned that in selected ion monitoring for S-lens optimization, compounds 112 and 119 were co-eluted (Fig. 5A) However, they produced different representative $MS^2$ spectra in MS/MS fragmentation, which were similar to those produced from their respective LTQ fragmentation. Peak 112 produced a predominant product at *m/z* 169.0 in both MS/MS and LTQ-Orbitrap $MS^2$ spectra (Fig. 5C and Fig. 5D), while peak 119 produced a product at *m/z* 301.2 (Fig. 5E and Fig. 5F). Therefore, the different resulting MRM transitions enable good separation of the two compounds in MS (Fig. 5B), indicating the advantages of the MRM method. Overall, for the 22 targeted analytes, flavonoid aglycones favored $^{1,3}A^+$, flavonoid *O*-glycosides favored aglycone ions, and the methoxylated flavonoids favored neutral loss of methyl radicals for monitoring, except in the case of peaks 98 and 112. Peak 98 lost two methyl radicals successively, while peak 112 produced abundant $^{1,3}A^+$ ions for monitoring. Peak 13 was identified as *C*-glycosides, of which $[M+H–138]^+$ was the favored product, while peak 22 favored product $[M+H–186]^+$. The optimized parameters are shown in Table 2.

**Application to the detection of exposure components in dosed plasma**

After optimizing the CE and S-lens parameters, the modified MRM method was applied to all dosed plasma samples. A signal to noise ratio of above 10 was identified as the limit of quantification (LOQ), and detection in more than 3 duplicate samples up to the LOQ was identified as an exposure component. Interestingly, all 22 compounds showed exposure *in vivo*, although some of them were only partially detected in the dosed plasma samples. The 22 exposure components were divided into two classes, short exposure time and long exposure time. Among them, peak 22 was detected at 0.17, 0.33, 050, 0.75, 1.0, and 2.0 h after administration. Peaks 133 143 were detected at 0.08, 0.17, 0.33, 050, 0.75, 1.0, 2.0, and 4.0 h. The exposure times of the three above-mentioned peaks were just below 4 h, which are expressed as mass response ratio–time plots. In contrast, all other peaks showed >12 h exposure time, which were conducted for next exposure level profiling (Fig. 6). Actually, flavonoid, compounds with three or more phenolic hydroxyl, has a poor water-solubility, which response for the relative low bioavailability. Additionally, comprehensive bio-transformation and metabolism in intestinal microflora and liver, especially, glycosylation or/and deglycosylation may in part explain the relative less peak detection in blood plasma.

**Investigation of relative exposure levels by pharmacokinetic analysis**

With the above observations in hand, we endeavored to profile the relative exposure levels of the long exposure time components. By using sequentially diluted original herbal preparations to prepare the "mixed calibration curves," herbal pharmacokinetics and relative exposure levels were successfully determined. To meet the analytical requirements, the developed MRM method was validated with respect to the linear dynamic range, precision, and accuracy. The results suggested that the improved method gave a sufficient dynamic range for all target analytes, with correlation coefficients exceeding 0.9997. The inter-batch and intra-batch precision RSD values were both below 15% in HPLC/MS-MS for all target analytes (Table 3). All validation experiments attest to the accuracy and reliability of this developed method for the simultaneous analysis of 19 flavonoids in plasma samples.

Using the "mixed calibration curves," the plasma concentration of each component was expressed as the relative concentration of the herbal extract. The concentration–time profiles are shown in Fig. 6 and estimated pharmacokinetic parameters are listed in Table 4. From this information, we concluded that all flavonoids exhibited rapid absorption, with $T_{max}$ values of approximately 20–40 min. Furthermore, with the exception of flavonoid *C*-glycosides, most flavones presented bimodal phenomena in agreement with prior reports[27, 28]. The evidence suggested that the first absorption site was likely due to direct absorption, while enteric glucuronidation metabolism from other aglycones and enterohepatic circulation may contribute to the second peak. Peaks 74, 91, and 92 presented the $C_{max}$ of the second peak, probably due to metabolic transformation from other aglycone compounds. Specifically, peak 88 at *m/z* 301.1 showed a continuously increasing concentration up to 10 h after administration. This noticeable phenomenon suggested that an extra transformation from other *O*-glycosides or glucuronides may be occurred. Relative exposure levels were described as $AUC_{0\text{-}t}$(component)/$AUC_{0\text{-}t}$(max), and we found that peaks 91, 142, and the 88 had high relative exposure levels.

**Comparison with HPLC/LTQ-Orbitrap-MS analysis**

As a comparison, we employed HPLC/LTQ-Orbitrap-MS for the detection of exposure components. Plasma samples collected at 4 and 10 h after intragastric

administration were subjected to HPLC/LTQ-Orbitrap-MS qualitative analysis. After matching the chemical peaks to the extract samples, it was striking that we detected only 12 components absorbed into the blood (supplementary information Fig. S3). High resolution MS has advantages in quantification. However, for quantitative analysis, especially of bio-samples, the complex matrixes certainly affect the detection of exposure compounds by using full mass scan monitoring. The endogenous substances, such as free fatty acids and lysophosphatidylcholines, being detected (*m/z* 200-600) in negative ionization mode, usually concealed low abundances exposure components. In contrast, the developed method using MRM transitions could sensitively detect exposure components. The matrix effect, detection sensitivity, dynamic range must be improved by comparison with that of high resolution MS. In conclusion, the improved MRM method exhibited high performance in profiling of exposure profiles in complex herbal systems, yielding exposure components, exposure times, and relative exposure levels.

**Analysis of *Tripterygium wilfordii Hook.F.* extract**

Having established the ability of our method to provide exposure profiling of *Scutellaria baicalensis*, we next sought to test the performance of this improved approach in the analysis of an unexplored herbal system. *Tripterygium wilfordii Hook.F.* is widely used for the treatment of rheumatoid arthritis, systemic lupus erythematosus, ankylosing spondylitis, and psoriasis. Pyridine alkaloids are considered to be the main effective and toxic components. *In vivo* exposure of these components would lead to improved understanding of their pharmacology and especially their toxicology. We applied our MRM method step-by-step to the detection of exposed pyridine alkaloids. Firstly, we conducted high resolution LTQ-Orbitrap-MS for the detection of pyridine alkaloids. A potential formula and component assignment could be provided by accurate mass detection. In this step, careful $MS^n$ fragmentation by LTQ and structural characterization were simplified and replaced by HPLC/MS-MS fragmentation later on in the procedure. From MS/MS fragmentation, products at *m/z* 177.9, 206.0, 176.1, and 194.1 unambiguously indicated pyridine alkaloid detection[29, 30]. Subsequently, full mass scan monitoring by HPLC/MS-MS was conducted, and a total of 55 components were screened out. Next, the MRM method was developed based on selected ion monitoring and product ion monitoring under chromatographic separation. The results are illustrated in Table 5. Using the current method, the MRM transition parameters of all 55 compounds were obtained and could be specifically detected in the dosed plasma samples. The MRM method was therefore applied successfully to all dosed plasma

samples. Thirty-nine peaks were identified as detectable exposure components, expressed as mass response ratio–time plots. Among them, 23 pyridine alkaloids had long exposure times (12–24 h), which can provide further pharmacokinetic behavior information. A further 8 had moderate exposure times (4–10 h), while the remainder had short exposure times (<4 h) (Fig. 7). These results independently confirmed that the modified MRM method is an efficient and powerful technique for *in vivo* exposure profiling of complex herbal systems.

## Conclusion

Lots herbal medicines exhibited good pharmacological effect. An notable example is artemisinin. Therefore, the investigation of exposure profile is important, and plays a significant role in the clarification of herbal efficacy. However, it is a bottleneck since the absent of the pure compounds. Our approach is developed to address it. Taking the advantages of sensitivity, this study reported the development of a modified MRM method that is expected to be universally applicable to the systemic investigation of exposure profiling in complex herbal systems. Unlike empirical detection based on high resolution MS techniques, investigating exposure components at several time points after administration, our developed approach provided a more comprehensive framework of exposure profiles independent of standards. Upon integration with the "relative exposure method," the improved approach offered a common solution for obtaining systemic exposure profiles *in vivo*, including exposure compounds, exposure times, and relative exposure levels. Our approach has been successfully validated as highly efficient and reliable in the detection of two homologous families in compound mixtures, and its use is anticipated in other complex exogenous or endogenous components, such as endogenous oxylipins.

## Acknowledgement

This study was financially supported by Natural Science Foundation of China (Grants No. 81303295, 81373688), Natural Science Foundation of Jiangsu Province, China (Grant No. BK20130959), The Specialized Research Fund for the Doctoral Program of Higher Education of China (Grant No. 20133237120001) and Colleges and universities in Jiangsu Province Natural Science Research (Grants No. 13KJB360005).

## Conflict of interest

On behalf of all authors, the corresponding author states that there is no conflict of interest.

## References


1. L. J. Liu, X. W. Wu, R. F. Wang, Y. S. Peng, X. Yang and J. X. Liu, *Chin. J. Nat. Med.*, 2014, **12**, 700-704.
2. G. K. Walkup, Z. You, P. L. Ross, E. K. Allen, F. Daryaee, M. R. Hale, J. O'Donnell, D. E. Ehmann, V. J. Schuck, E. T. Buurman, A. L. Choy, L. Hajec, K. Murphy-Benenato, V. Marone, S. A. Patey, L. A. Grosser, M. Johnstone, S. G. Walker, P. J. Tonge and S. L. Fisher, *Nat. Chem. Biol.*, 2015, **11**, 416-423.
3. R. A. Copeland, D. L. Pompliano and T. D. Meek, *Nat. Rev. Drug Discov.*, 2006, **5**, 730-739.
4. H. Lu and P. J. Tonge, *Curr. Opin. Chem. Biol.*, 2010, **14**, 467-474.
5. P. Gong, N. Cui, L. Wu, Y. Liang, K. Hao, X. Xu, W. Tang, G. Wang and H. Hao, *Anal. Chem.*, 2012, **84**, 2995-3002.
6. Y. Liang, H. Hao, L. Xie, A. Kang, T. Xie, X. Zheng, C. Dai, K. Hao, L. Sheng and G. Wang, *Drug Metab. Dispos.*, 2010, **38**, 1747-1759.
7. Y. Chen, J. Guo, Y. Tang, L. Wu, W. Tao, Y. Qian and J. A. Duan, *J. Pharm. Biomed. Anal.*, 2015, **112**, 60-69.
8. R. Zuo, W. Ren, B. L. Bian, H. J. Wang, Y. N. Wang, H. Hu, H. Y. Zhao and N. Si, *Xenobiotica,* 2015, DOI: 10.3109/00498254.2015.1048541, 1-17.
9. A. Taamalli, D. Arraez-Roman, L. Abaza, I. Iswaldi, A. Fernandez-Gutierrez, M. Zarrouk and A. Segura-Carretero, *Phytochem. Anal.*, 2015, **26,** 320-330.
10. X.-W. Liu, F. Zhang, S.-H. Gao, B. Jiang and W.-S. Chen, *Chin. J. Nat. Med.*, 2015, **13**, 145-160.
11. M. Liu, P. Li, X. Zeng, H. Wu, W. Su and J. He, *Int. J. Mol. Sci.*, 2015, **16**, 5047-5071.
12. Y. N. Tang, Y. X. Pang, X. C. He, Y. Z. Zhang, J. Y. Zhang, Z. Z. Zhao, T. Yi and H. B. Chen, *J. Ethnopharmacol.*, 2015, **165**, 127-140.
13. Y. Liang, H. Hao, A. Kang, L. Xie, T. Xie, X. Zheng, C. Dai, L. Wan, L. Sheng and G. Wang, *J. Chromatogr. A*, 2010, **1217**, 4971-4979.
14. M. Mazzarino, X. de la Torre and F. Botrè, *Anal. Bioanal. Chem.*, 2008, **392**, 681-698.
15. M. Razavi, L. E. Frick, W. A. LaMarr, M. E. Pope, C. A. Miller, N. L. Anderson and T. W. Pearson, *J. Proteome Res.*, 2012, **11**, 5642-5649.
16. Z. Li, S. Xiao, N. Ai, K. Luo, X. Fan and Y. Cheng, *J. Chromatogr. A*,, 2015, **1376**, 126-142.
17. V. Vukics and A. Guttman, *Mass Spectrom. Rev.*, 2010, **29**, 1-16.
18. Y. L. Ma, Q. M. Li, H. Van den Heuvel and M. Claeys, *Rapid Commun. Mass Spectrom.*, 1997, **11**, 1357-1364.
19. N. Fabre, I. Rustan, E. de Hoffmann and J. Quetin-Leclercq, *J. Am. Soc. Mass Spectrom.*, 2001, **12**, 707-715.

20. J. Y. Zhang, N. Li, Y. Y. Che, Y. Zhang, S. X. Liang, M. o. Zhao, Y. Jiang and P. e. Tu, *J Pharm. Biomed. Anal.*, 2011, **56**, 950-961.
21. B. Abad-García, S. Garmón-Lobato, L. A. Berrueta, B. Gallo and F. Vicente, *Rapid Commun. Mass Spectrom.*, 2008, **22**, 1834-1842.
22. R. Colombo, J. H. Yariwake and M. McCullagh, *J. Braz. Chem. Soc.*, 2008, **19**, 483-490.
23. O. Talhi and A. M. S. Silva, *Curr. Org. Chem.*, 2012, **16**, 859-896.
24. H. Wang, J. Cao, S. Xu, D. Gu, Y. Wang and S. Xiao, *J Chromatogr A*, 2013, **1315**, 107-117.
25. L. Chankvetadze, N. Ghibradze, M. Karchkhadze, L. Peng, T. Farkas and B. Chankvetadze, *J. Chromatogr. A*, 2011, **1218**, 6554-6560.
26. Q. Wang, Y. Xiong, B. Lu, J. Fan, S. Zhang, S. Zheng and W. Zhang, *J. Sep. Sci.*, 2013, **36**, 1343-1348.
27. L. Tong, M. Wan, L. Zhang, Y. Zhu, H. Sun and K. Bi, *J. Pharm. Biomed. Anal.*, 2012, **70**, 6-12.
28. T. Lu, J. Song, F. Huang, Y. Deng, L. Xie, G. Wang and X. Liu, *J. Ethnopharmacol.*, 2007, **110**, 412-418.
29. L. Qu, Y. Xiao, Z. Jia, Z. Wang, C. Wang, T. Hu, C. Wu and J. Zhang, *J. Chromatogr. A*, 2015, **1400**, 65-73.
30. M. X. Su, M. Song, D. S. Yang, J. F. Shi, B. Di and T. J. Hang, *J. Chromatogr. B Analyt. Technol. Biomed. Life Sci.*, 2015, **990**, 31-38.

**Figure captions**

**Fig. 1** Total ion chromatograms of *Scutellaria baicalensis* extract obtained by HPLC/LTQ-Orbitrap-MS: (A) in positive ionization mode; (B) in negative ionization mode; (C) total ion chromatogramS of *Scutellaria baicalensis* extract obtained based on full mass scan monitoring by HPLC/MS-MS

**Fig. 2** The structures of characterized flavonoids in *Scutellaria baicalensis* extract by HPLC/LTQ-Orbitrap-MS

**Fig. 3** (A) Total ion chromatograms of product ion monitoring from *m/z* 549.2 by HPLC/MS-MS; (B) the peak 13 in LTQ-Orbitrap-MS give the similar $MS^2$ spectrum with (C) that of the peak *m/z* 549.2 eluted at 1.78 min in HPLC/MS-MS with CE 18eV; (D-H) the $MS^2$ spectra with different CE values in HPLC/MS-MS.

**Fig. 4** The extracted ion chromatograms of *m/z* 549.2 by selected ion monitoring at different S-lens values

**Fig. 5** (A) Peak 112 and 119 were co-eluted in the extracted ion chromatograms of *m/z* 331.2 by selected ion monitoring; however, (B) two peaks can be well separated using different MRM transitions in this developed method; the similar $MS^2$ spectra of peak 112 between (C) MS/MS and (D) LTQ-Orbitrap-MS produced predominant product at *m/z* 169.0; and the similar $MS^2$ spectra of peak 119 between (E) MS/MS and (F) LTQ-Orbitrap-MS produced predominant product at *m/z* 301.2

**Fig. 6** The exposure levels of 22 detected flavones *in vivo.* Peak 133, 143, 22 present short exposure time, expressing as mass response ration-time plot. Other peaks present long exposure time, expressing as relative concentration- time plot by "relative exposure method"

**Fig. 7** The exposure time of the exposure pyridine alkaloids in *Tripterygium wilfordii Hook.F.*. According to exposure time, the components can be divided into short exposure components, moderate exposure components, and long exposure components

353 Table 1 The peaks detection and identification by HPLC/MS-MS

| *m/z* | $t_R$(min) | CE(eV) | Characteristic fragments by HPLC/MS-MS | Matched with LTQ-Orbitrap | Identification |
|---|---|---|---|---|---|
| 549.2 | 1.78 | 25 | 279.1, 309.0, 363.1, 375.1, 393.1, 411.1, 429.2, 459.1, 465.1, 483.2, 495.2, 513.2, 531.2, 549.2 | Peak 13 | chrysin 6-*C*-arabinoside 8-*C*-glucoside |
| 549.2 | 1.96 | 25 | 279.0, 291.1, 309.1, 321.1, 345.1, 363.1, 375.1, 381.1, 387.1, 393.1, 399.2, 411.1, 429.1, 435.1, 441.1, 465.2, 477.2, 495.2, 513.4 | Peak 22 | chrysin 6-*C*-glucoside 8-*C*-arabinoside |
| 447.2 | 3.75 | 45 | 123.0, 169.0, 197.0, 211.0, 225.1, 253.0, 271.0 | Peak 58 | baicalin* |
| 317.1 | 4.34 | 40 | 112.2, 136.4, 139.9, 168.1, 182.9, 268.0, 211.0, 256.4, 273.2, 302.0 | Peak 61 | 5,7,3',4'-tetrahydroxy-8-methoxy flavone |
| 447.2 | 4.76 | 45 | 123.1, 128.9, 141.1, 150.9, 169.0, 214.9, 224.9, 253.0, 271.0 | Peak 74 | norwogonin *O*-glucuronide |
| 461.2 | 4.96 | - | - | Peak 83 | orxy A* |
| 301.1 | 4.97 | 40 | 128.0, 138.0, 156.0, 171.1, 184.0, 212.1, 228.7, 240.2, 269.1, 286.2 | Peak 88 | 5,6,8-trihydroxy-7-methoxy flavone |
| 447.2 | 5.40 | 45 | 123.1, 128.9, 141.1, 150.9, 169.0, 214.9, 224.9, 253.0, 271.0 | Peak 91 | baicalein *O*-glucuronide |
| 461.2 | 5.42 | - | - | Peak 92 | wogonside* |
| 315.1 | 5.48 | 30 | 179.9, 183.0, 198.1, 213.2, 225.0, 254.1, 282.0, 285.0, 300.0, 315.2 | Peak 98 | 5,8-dihydroxy-6,7-dimethoxy flavone |
| 301.1 | 5.84 | 30 | 140.0, 160.0, 168.1, 184.0, 195.0, 216.2, 239.9, 257.1, 268.0, 286.0 | Peak 100 | 5,6,8-trihydroxy-7-methoxy flavone |
| 331.1 | 5.90 | 30 | 155.2, 182.9, 197.2, 212.9, 228.0, 243.1, 271.0, 285.2, 298.0, 301.0 | Peak 106 | 5,2',6'-trihydroxy-7,8-dimethoxy flavone |
| 331.1 | 6.34 | 20 | 142.0, 169.0, 182.9, 228.1, 239.0, 271.0, 298.0, 316.1, 331.1 | Peak 112 | 5,7,2'-trihydroxy-8,6'-dimethoxy flavone |
| 331.1 | 6.43 | 20 | 169.0, 180.0, 182.9, 214.2, 242.2, 273.1, 298.0, 301.0, 316.1, 331.1 | Peak 119 | 5,6,2'-trihydroxy-7,8-dimethoxy flavone |
| 301.1 | 6.55 | 40 | 112.0, 121.0, 140.0, 168.0, 229.1, 239.1, 257.9, 268.7, 286.0 | Peak 121 | 5,7,2'-trihydroxy-6-methoxy flavone |
| 271.2 | 6.56 | - | - | Peak 120 | baicalein* |
| 345.2 | 7.47 | 25 | 165.1, 183.0, 197.0, 269.0, 284.0, 301.0, 312.1, 315.1, 330.0, 345.1 | Peak 133 | 5,2'-dihydroxy-7,8,6'-trimethoxy flavone |
| 285.2 | 7.61 | - | - | Peak 134 | wogonin* |
| 375.1 | 7.72 | 30 | 149.1, 169.0, 197.0, 212.0, 227.0, 299.1, 327.1, 345.1, 360.1, 375.2 | Peak 140 | 5,2'-dihydroxy-6,7,8,6'-tetramethoxy flavone |
| 315.2 | 7.74 | 40 | 103.1, 155.0, 183.0, 198.1, 257.0, 282.1, 285.1, 300.0 | Peak 142 | 5,2'-dihydroxy-7,8-dimethoxy flavone |
| 285.2 | 7.91 | - | - | Peak 139 | oroxylin A* |
| 345.2 | 8.10 | 30 | 151.0, 169.0, 178.9, 197.0, 227.0, 287.0, 297.1, 315.1, 330.0, 345.2 | Peak 143 | 5,2'-dihydroxy-6,7,8-trimethoxy flavone |

354 * The compounds were characterized by standards

355 Table 2 The optimization of CE and S-lens based on HPLC/MS-MS to obtain the MRM transition parameters

| Peak | Comparison of CE voltages (%) | | | | | | Comparison of S-lens voltages (%) | | | | | | | MRM transition |
|---|---|---|---|---|---|---|---|---|---|---|---|---|---|---|
| No. | 18eV | 20eV | 22eV | 25eV | 28eV | 30eV | 60V | 70V | 80V | 90V | 100V | 110V | 120V | (S-lens/V, CE/eV) |
| 13 | 100.0 | 80.4 | 65.5 | 49.6 | 28.6 | 21.7 | 85.5 | 96.3 | 94.6 | 96.2 | 100.0 | 86.9 | 82.9 | 549.2→411.1(100, 18) |
| 22 | 40.0 | 54.1 | 78.5 | 83.8 | 100.0 | 99.6 | 94.4 | 98.7 | 91.3 | 100.0 | 97.6 | 79.5 | 75.3 | 549.2→363.1(90, 28) |
| 58 | - | 62.3 | 79.6 | 100.0 | 97.0 | 55.1 | 85.5 | 90.0 | 96.4 | 100.0 | 88.5 | 72.4 | 52.3 | 447.2→271.1(90, 25) |
| 61 | - | 47.1 | 70.4 | 98.8 | 100.0 | 84.6 | 69.2 | 71.8 | 81.8 | 100.0 | 99.0 | 96.5 | 89.9 | 317.2→302.1(90, 28) |
| 74 | - | 75.1 | 98.8 | 100.0 | 81.1 | 95.5 | 90.2 | 86.9 | 100.0 | 91.1 | 91.2 | 89.2 | 79.4 | 447.2→271.1(80, 25) |
| 83 | Optimization by direct infusion of standard | | | | | | | | | | | | | 461.2→285.1(88, 19) |
| 88 | - | 73.3 | 100.0 | 76.1 | 86.9 | 56.6 | 68.6 | 74.4 | 85.1 | 96.6 | 100.0 | 92.9 | 81.1 | 301.2→286.1(100, 25) |
| 91 | - | 100.0 | 86.7 | 91.7 | 83.1 | 80.1 | 94.8 | 100.0 | 90.0 | 79.2 | 60.8 | 35.2 | 26.4 | 447.2→271.1(70, 25) |
| 92 | Optimization by direct infusion of standard | | | | | | | | | | | | | 461.2→285.1(88, 19) |
| 98 | - | 59.6 | 76.5 | 100.0 | 88.8 | 82.4 | 15.4 | 28.6 | 34.5 | 53.0 | 69.6 | 83.8 | 100.0 | 315.2→285.1(120, 25) |
| 100 | - | 65.1 | 78.6 | 100.0 | 89.3 | 55.1 | 72.5 | 77.1 | 88.6 | 94.6 | 100.0 | 97.3 | 93.4 | 301.2→286.1(100, 25) |
| 106 | - | 51.0 | 91.3 | 88.5 | 84.5 | 100.0 | 73.6 | 76.33 | 96.18 | 99.25 | 100.0 | 96.3 | 95.5 | 331.2→301.1(100, 25) |
| 112 | - | 33.6 | 53.3 | 71.8 | 100.0 | 98.3 | 67.4 | 74.8 | 84.8 | 94.7 | 100.0 | 9.7 | 92.3 | 331.2→169.1(100, 28) |
| 119* | - | 50.7 | 71.3 | 49.5 | 55.9 | 100.0 | - | - | - | - | - | - | - | 331.2→301.1(100, 25) |
| 121 | - | 77.9 | 85.7 | 100.0 | 76.8 | 56.6 | 69.4 | 75.7 | 89.6 | 97.8 | 100.0 | 92.88 | 79.9 | 301.2→286.1(100, 25) |
| 120 | Optimization by direct infusion of standard | | | | | | | | | | | | | 271.2→123.1(114, 32) |
| 133 | - | 52.0 | 59.7 | 82.2 | 89.3 | 100.0 | 69.1 | 70.57 | 89.9 | 97.1 | 100.0 | 99.58 | 94.4 | 345.2→315.1(100, 30) |
| 134 | Optimization by direct infusion of standard | | | | | | | | | | | | | 285.2→270.1(82, 23) |
| 140 | - | 48.3 | 66.3 | 100.0 | 89.0 | 92.2 | 61.2 | 70.98 | 81.3 | 93.7 | 100.0 | 91.9 | 90.7 | 375.2→345.1(100, 30) |
| 142 | - | 57.3 | 74.2 | 99.0 | 100.0 | 86.4 | 63.8 | 72.7 | 81.9 | 96.6 | 100.0 | 92.8 | 88.4 | 315.2→285.1(100, 25) |
| 139 | Optimization by direct infusion of standard | | | | | | | | | | | | | 285.2→270.1(82, 23) |
| 143 | - | 50.8 | 63.1 | 100.0 | 97.4 | 82.4 | 63.3 | 70.0 | 81.7 | 92.0 | 100.0 | 95.4 | 90.3 | 345.2→315.1(100, 25) |

356 * Peak 119 and 112 were co-eluted. Peak integration of two peaks was combined when optimizing of S-lens parameters.

357

358 Table 3 Data for linearity, regression equation, accuracy and precision of the method.

| Peak No. | Linearity (mg/mL) | Regression equation | $r^2$ | Intra-day (%)/Added amount (mg/mL) | | | | | | Inter-day (%)/Added amount (mg/mL) | | | | | |
|---|---|---|---|---|---|---|---|---|---|---|---|---|---|---|---|
| | | | | 0.0195 | | 0.1563 | | 1.250 | | 0.0195 | | 0.1563 | | 1.250 | |
| | | | | RSD | RE | RSD | RE | RSD | RE | RSD | RE | RSD | RE | RSD | RE |
| 13 | 0.01-2.5 | y = 34.388x+0.074 | 0.9999 | 13.11 | 2.94 | 10.49 | 4.11 | 4.96 | 0.39 | 8.94 | 4.11 | 8.40 | 1.99 | 4.68 | 1.39 |
| 58 | 0.01-5 | y = 1521.5x-11.44 | 0.9998 | 5.51 | -7.62 | 10.45 | 8.44 | 6.09 | -1.09 | 6.10 | -14.58 | 8.32 | 4.96 | 7.46 | -11.00 |
| 61 | 0.01-5 | y = 4.1561x+0.004 | 1.0000 | 14.73 | 8.55 | 11.97 | 4.59 | 6.13 | 0.66 | 10.74 | 8.62 | 14.83 | 0.37 | 7.87 | -8.63 |
| 74 | 0.01-1.25 | y = 225.56x+0.73 | 1.0000 | 11.90 | 4.64 | 7.49 | 2.41 | 4.76 | 3.56 | 11.47 | -0.47 | 10.85 | -5.05 | 7.43 | -4.90 |
| 83 | 0.0195-2.5 | y = 342.62x+2.336 | 1.0000 | 12.10 | 10.18 | 7.26 | 5.78 | 2.96 | 3.05 | 12.32 | -2.65 | 11.88 | -2.07 | 6.41 | -3.72 |
| 88 | 0.0195-5 | y = 16.377x -0.015 | 1.0000 | 8.15 | -1.86 | 9.92 | 9.30 | 5.83 | -1.16 | 9.29 | -13.16 | 13.46 | -1.25 | 4.14 | 0.71 |
| 91 | 0.0195-1.25 | y = 56.074x-0.000 | 0.9999 | 4.61 | -8.70 | 8.13 | -2.76 | 0.97 | 0.51 | 9.38 | -9.45 | 9.69 | -1.23 | 2.44 | 2.03 |
| 92 | 0.01-1.25 | y = 2272x+4.752 | 0.9999 | 8.77 | 0.81 | 5.29 | 3.80 | 1.86 | -2.12 | 8.06 | -3.69 | 10.90 | -3.77 | 2.74 | -0.91 |
| 98 | 0.01-1.25 | y = 32.769x+0.275 | 0.9998 | 4.86 | 8.43 | 6.04 | -1.64 | 5.22 | 8.00 | 9.67 | -1.95 | 7.03 | -9.59 | 8.57 | -2.82 |
| 100 | 0.039-5 | y = 34.831x-0.388 | 1.0000 | 5.95 | -2.55 | 6.50 | 5.05 | 3.94 | 5.35 | 6.58 | -5.61 | 7.50 | 3.92 | 5.21 | -0.56 |
| 106 | 0.039-5 | y = 2.6559x-0.002 | 0.9997 | 9.07 | 0.72 | 6.04 | 5.48 | 0.47 | -1.10 | 8.01 | -4.52 | 7.43 | 4.06 | 3.57 | -2.10 |
| 112 | 0.039-5 | y = 14.715x+0.023 | 0.9998 | 7.54 | 2.60 | 3.85 | 2.53 | 5.79 | 1.57 | 8.10 | -3.89 | 9.54 | 4.93 | 5.68 | -3.57 |
| 119 | 0.0195-2.5 | y = 16.098x-0.214 | 0.9999 | 6.67 | 2.60 | 9.53 | 2.56 | 4.01 | 1.96 | 6.56 | -0.82 | 7.56 | 1.55 | 3.10 | -0.72 |
| 121 | 0.0195-2.5 | y = 49.337x-0.269 | 0.9999 | 9.60 | 0.74 | 9.53 | 2.56 | 4.01 | 1.96 | 9.83 | 3.25 | 6.46 | 0.07 | 3.10 | -0.72 |
| 120 | 0.0195-2.5 | y = 43.192x+0.847 | 0.9998 | 7.52 | -10.41 | 7.48 | 6.93 | 1.16 | 3.24 | 10.60 | -13.31 | 10.09 | 4.83 | 6.18 | 7.91 |
| 134 | 0.01-1.25 | y = 1497.5x-9.964 | 0.9999 | 7.68 | -5.30 | 4.06 | 5.06 | 3.92 | -2.33 | 11.87 | -10.39 | 9.96 | 6.82 | 3.98 | -5.96 |
| 140 | 0.0195-2.5 | y = 137.84x-0.209 | 1.0000 | 11.37 | 0.50 | 7.57 | 6.87 | 0.76 | -5.89 | 8.62 | -7.21 | 8.69 | 4.10 | 2.93 | -7.61 |
| 142 | 0.0195-5 | y = 78.422x-0.174 | 0.9999 | 14.40 | 4.38 | 8.46 | 9.51 | 2.69 | -5.46 | 10.51 | -0.58 | 8.44 | 5.35 | 3.95 | -9.14 |
| 139 | 0.01-2.5 | y = 828.25x-0.03 | 0.9998 | 11.59 | -0.43 | 11.62 | 8.29 | 2.54 | -5.86 | 8.38 | -4.60 | 8.77 | 3.85 | 3.97 | -9.61 |

359
360
361
362

363 Table 4 Pharmacokinetic parameters of the exposure components by "relative exposure method"

| Parameters | $C_{max}$ (mg/mL) | $T_{max}$ (h) | $T_{bimodal}$ (h) | $AUC_{0-t}$ ($mg \cdot h \cdot mL^{-1}$) | $AUMC_{0-t}$ ($mg \cdot h^2 \cdot mL^{-1}$) | $MRT_{0-t}$ (h) | $t_{1/2}$ (h) | REP** (%) |
|---|---|---|---|---|---|---|---|---|
| 13 | 0.33±0.20 | 0.67±0.26 | | 1.32±0.40 | 10.09±3.12 | 7.71±1.42 | 20.71±8.99 | 0.26 |
| 58 | 0.57±0.20 | 0.65±0.22 | 8.00±2.00 | 6.54±1.57 | 85.12±23.68 | 12.91±0.93 | 12.96±3.61 | 1.29 |
| 61 | 0.59±0.25 | 0.86±0.62 | 9.20±1.79 | 2.09±0.75 | 16.92±5.44 | 8.31±1.24 | 7.21±1.35 | 0.41 |
| 74* | 2.15±0.58 | 0.90±0.63 | 9.60±1.67 | 32.62±5.74 | 491.69±103.17 | 15.00±0.66 | - | 6.44 |
| 83* | 1.19±0.50 | 0.75±0.25 | 10.00±1.41 | 11.98±2.45 | 171.58±54.23 | 14.19±2.06 | - | 2.37 |
| 91 | 39.17±11.33 | 1.05±0.57 | 8.80±2.28 | 506.36±113.26 | 6517.47±1593.65 | 12.83±0.64 | 7.36±1.34 | 100.00 |
| 92* | 0.40±0.07 | 0.55±0.33 | 10.33±0.82 | 6.76±1.96 | 106.21±35.10 | 15.75±1.83 | - | 1.34 |
| 98* | 0.99±0.36 | 0.88±0.14 | 10.40±2.61 | 16.80±6.22 | 250.54±99.55 | 15.17±1.74 | - | 3.32 |
| 88 | 10.67±2.4 | 1.13±0.60 | 11.20±1.79 | 215.94±28.33 | 3240.63±499.68 | 14.99±0.83 | 14.23±3.03 | 42.65 |
| 100 | 1.77±0.87 | 0.63±0.26 | 9.33±2.42 | 7.00±2.43 | 68.23±26.17 | 9.58±1.53 | 8.11±3.13 | 1.38 |
| 106 | 4.53±2.95 | 0.67±0.20 | 8.50±3.00 | 18.16±2.97 | 171.52±30.77 | 9.52±1.66 | 28.56±16.50 | 3.59 |
| 112 | 2.94±1.68 | 0.61±0.29 | 9.20±2.28 | 15.01±2.98 | 162.71±42.18 | 11.25±2.16 | 12.35±6.03 | 2.96 |
| 119 | 1.06±0.67 | 0.53±0.21 | 10.50±1.91 | 5.77±2.94 | 62.98±32.74 | 10.82±1.56 | 9.74±5.20 | 1.14 |
| 121 | 1.68±1.29 | 0.47±0.26 | 10.50±3.21 | 7.50±3.36 | 86.78±38.03 | 11.33±2.10 | 6.54±2.67 | 1.48 |
| 120 | 0.89±0.57 | 0.45±0.27 | 9.67±2.94 | 4.22±2.34 | 47.35±26.16 | 11.51±2.23 | 8.95±5.56 | 0.83 |
| 134* | 2.08±0.75 | 0.38±0.24 | 9.60±1.67 | 15.63±4.88 | 181.25±57.31 | 11.58±0.82 | - | 3.09 |
| 140 | 0.15±0.04 | 0.34±0.28 | 7.50±1.91 | 0.82±0.15 | 9.84±1.88 | 12.02±1.72 | 22.26±8.70 | 0.16 |
| 142 | 13.09±6.49 | 0.75±0.25 | 10.50±1.00 | 91.47±27.93 | 1056.75±340.93 | 11.52±0.93 | 7.87±1.08 | 18.06 |
| 139 | 4.21±2.01 | 0.43±0.29 | 10.00±1.41 | 15.01±5.04 | 138.34±44.72 | 9.25±1.56 | 14.47±10.58 | 2.96 |

364 *$t_{1/2}$ can not be calculated because of inadequacy data of the elimination phase

365 ** REP: Relative exposure levels were described as the ratio $AUC_{0-t}$(component)/$AUC_{0-t}$(max)

Table 5 Detection and parameter optimization of detected peaks in *Tripterygium wilfordii Hook.F.* extract

| | HPLC/MS-MS | | | HPLC/LTQ-Orbitrap | | | |
|---|---|---|---|---|---|---|---|
| No. | $t_R$ (min) | MRM transition (S-lens/V, CE/eV) | Characteristic products | $t_R$ (min) | m/z | Predict formula | ppm |
| 1 | 4.91 | 738.3→175.5(140, 45) | 175.5, 193.8 | 5.77 | 738.2588 | $C_{34}H_{44}O_{17}N$ | -1.59 |
| 2 | 5.15 | 738.3→175.5(140, 45) | 175.5, 193.8 | 6.06 | 738.2587 | $C_{34}H_{44}O_{17}N$ | -1.65 |
| 3 | 5.36 | 738.3→175.5(140, 45) | 175.5, 193.8 | 6.40 | 738.2590 | $C_{34}H_{44}O_{17}N$ | -1.35 |
| 4 | 5.62 | 738.3→175.5(140, 45) | 175.5, 193.8 | 6.62 | 738.2590 | $C_{34}H_{44}O_{17}N$ | -1.35 |
| 5 | 5.71 | 738.3→175.5(140, 45) | 175.5, 193.8 | 6.71 | 738.2577 | $C_{34}H_{44}O_{17}N$ | -2.69 |
| 6 | 6.32 | 764.3→205.5(140, 45) | 177.6, 205.7 | 7.50 | 764.2747 | $C_{36}H_{46}O_{17}N$ | -1.37 |
| 7 | 6.73 | 764.3→205.5(140, 45) | 177.6, 205.7 | 7.71 | 764.2763 | $C_{36}H_{46}O_{17}N$ | 0.23 |
| 8 | 7.16 | 764.3→205.5(140, 45) | 177.6, 205.7 | 7.22 | 764.2747 | $C_{36}H_{46}O_{17}N$ | -1.31 |
| 9 | 6.82 | 774.3→205.6(140, 45) | 177.9, 205.8 | 7.58 | 774.2226 | $C_{36}H_{40}O_{18}N$ | -1.39 |
| 10 | 7.23 | 774.3→205.6(140, 45) | 177.9, 205.8 | 8.24 | 774.2592 | $C_{37}H_{44}O_{17}N$ | -1.22 |
| 11 | 7.48 | 774.3→205.6(140, 45) | 177.9, 205.8 | 8.51 | 774.2594 | $C_{37}H_{44}O_{17}N$ | -0.98 |
| 12 | 7.65 | 774.3→205.6(140, 45) | 177.9, 205.8 | 8.55 | 774.2601 | $C_{37}H_{44}O_{17}N$ | -0.31 |
| 13 | 7.27 | 788.3→205.6(200, 45) | 177.9, 205.8 | 8.30 | 788.2738 | $C_{38}H_{46}O_{17}N$ | -2.23 |
| 14 | 6.24 | 796.3→175.6(140, 50) | 175.8, 193.8 | 7.17 | 796.2642 | $C_{36}H_{46}O_{19}N$ | -1.63 |
| 15 | 6.63 | 796.3→175.6(140, 50) | 175.8, 193.8 | 7.54 | 796.2649 | $C_{36}H_{46}O_{19}N$ | -0.96 |
| 16 | 6.62 | 806.3→205.9(140, 45) | 177.9, 206.0 | 7.43 | 806.2487 | $C_{37}H_{44}O_{19}N$ | -1.54 |
| 17 | 6.90 | 806.3→205.9(140, 45) | 177.9, 205.9 | 7.88 | 806.2862 | $C_{38}H_{48}O_{18}N$ | -0.40 |
| 18 | 7.09 | 806.3→205.9(140, 45) | 177.9, 205.9 | 8.09 | 806.2866 | $C_{38}H_{48}O_{18}N$ | -0.03 |
| 19 | 7.27 | 806.3→205.9(140, 45) | 177.9, 205.9 | 8.30 | 806.2866 | $C_{38}H_{48}O_{18}N$ | -0.03 |
| 20 | 6.24 | 818.3→177.7(140, 45) | 177.7, 193.8 | 7.20 | 818.2469 | $C_{38}H_{44}O_{19}N$ | -3.31 |
| 21 | 6.62 | 818.3→123.9(140, 40) | 123.9 | 7.57 | 818.2509 | $C_{38}H_{44}O_{19}N$ | 0.72 |
| 22 | 6.43 | 822.3→133.7(140, 50) | 133.6, 151.4 | 7.38 | 822.2800 | $C_{38}H_{48}O_{19}N$ | -1.53 |
| 23 | 6.64 | 822.3→175.7(140, 55) | 176.1, 194.1 | 7.59 | 822.2814 | $C_{38}H_{48}O_{19}N$ | -0.13 |
| 24 | 8.10 | 826.3→205.7(140, 40) | 178.0, 205.9 | 9.15 | 826.2905 | $C_{41}H_{48}O_{17}N$ | -1.21 |
| 25 | 5.89 | 840.3→176.0(140, 50) | 176.1, 194.1 | 6.80 | 840.2902 | $C_{38}H_{50}O_{20}N$ | -1.91 |
| 26 | 6.19 | 840.3→176.0(140, 50) | 176.1, 194.1 | 7.13 | 840.2918 | $C_{38}H_{50}O_{20}N$ | -0.26 |
| 27 | 6.55 | 850.3→239.5(140, 35) | 176.0, 194.0 | 7.53 | 850.2743 | $C_{39}H_{48}O_{20}N$ | -2.13 |
| 28 | 7.64 | 858.3→205.8(140, 45) | 178.0, 205.9 | 8.66 | 858.2813 | $C_{41}H_{48}O_{19}N$ | -0.25 |
| 29 | 7.79 | 858.3→205.8(140, 45) | 178.0, 205.9 | 8.81 | 858.2805 | $C_{41}H_{48}O_{19}N$ | -0.98 |
| 30 | 8.03 | 858.3→205.8(140, 45) | 178.0, 205.9 | 8.98 | 858.2802 | $C_{41}H_{48}O_{19}N$ | -1.35 |
| 31 | 8.12 | 868.4→205.7(160, 45) | 177.8, 206.1 | 9.18 | 868.3015 | $C_{43}H_{50}O_{18}N$ | -0.79 |
| 32 | 8.4 | 868.4→205.7(160, 45) | 178.0, 205.5 | 9.52 | 868.3007 | $C_{43}H_{50}O_{18}N$ | -1.58 |
| 33 | 7.22 | 874.3→205.9(160, 45) | 178.0, 205.9 | 8.23 | 874.2748 | $C_{41}H_{48}O_{20}N$ | -1.64 |
| 34 | 7.49 | 874.3→175.9(140, 45) | 176.1, 194.1 | 8.52 | 874.2765 | $C_{41}H_{48}O_{20}N$ | 0.07 |
| 35 | 7.69 | 884.3→133.5(140, 50) | 133.5, 151.5 | 8.74 | 884.2956 | $C_{43}H_{50}O_{19}N$ | -1.56 |
| 36 | 8.01 | 884.3→175.5(140, 55) | 175.5, 193.5 | 9.07 | 884.2970 | $C_{43}H_{50}O_{19}N$ | -0.15 |
| 37 | 7.07 | 890.3→205.4(140, 50) | 177.8, 206.1 | 8.07 | 890.3058 | $C_{42}H_{52}O_{20}N$ | -1.93 |
| 38 | 6.12 | 892.4→175.3(140, 50) | 176.1, 194.1 | 7.08 | 892.2849 | $C_{41}H_{50}O_{21}N$ | -2.07 |
| 39 | 6.61 | 892.4→205.6(140, 50) | 177.8, 206.1 | 7.51 | 892.2844 | $C_{41}H_{50}O_{21}N$ | -2.56 |

| | | | | | | | |
|---|---|---|---|---|---|---|---|
| 40 | 7.02 | 892.4→175.5(140, 50) | 175.5, 193.8 | 8.02 | 892.2862 | $C_{41}H_{50}O_{21}N$ | -0.79 |
| 41 | 6.34 | 902.4→175.5(140, 40) | 175.5, 193.5 | 7.39 | 902.3069 | $C_{43}H_{52}O_{20}N$ | -0.84 |
| 42 | 7.47 | 902.4→175.5(140, 40) | 175.5, 193.5 | 8.49 | 902.3054 | $C_{43}H_{52}O_{20}N$ | -2.30 |
| 43 | 7.49 | 916.3→205.9(160, 55) | 177.7, 205.7 | 8.42 | 916.3232 | $C_{44}H_{54}O_{20}N$ | -0.19 |
| 44 | 7.64 | 916.3→205.9(160, 55) | 177.7, 205.7 | 8.66 | 916.3219 | $C_{44}H_{54}O_{20}N$ | -1.47 |
| 45 | 7.30 | 916.3→804.5(140, 30) | 203.9, 804.5 | 8.28 | 916.2820 | $C_{43}H_{50}O_{21}N$ | -4.94 |
| 46 | 7.47 | 924.3→177.5(140, 50) | 177.5, 200.5 | 8.50 | 924.2871 | $C_{45}H_{50}O_{20}N$ | -4.96 |
| 47 | 7.62 | 926.3→203.7(140, 50) | 203.5, 804.5 | 8.66 | 926.3066 | $C_{45}H_{52}O_{20}N$ | -1.08 |
| 48 | 7.23 | 932.3→205.5(140, 45) | 178.0, 205.9 | 8.23 | 932.3154 | $C_{44}H_{54}O_{21}N$ | -2.91 |
| 49 | 7.47 | 932.3→205.5(140, 45) | 178.0, 205.9 | 8.50 | 932.3148 | $C_{44}H_{54}O_{21}N$ | -3.46 |
| 50 | 8.00 | 946.3→205.5(160, 45) | 177.8, 205.7 | 9.05 | 946.3317 | $C_{45}H_{56}O_{21}N$ | -2.26 |
| 51 | 6.72 | 948.3→133.8(180, 50) | 133.5, 151.5 | 7.71 | 948.3123 | $C_{44}H_{54}O_{22}N$ | -0.88 |
| 52 | 7.36 | 948.3→205.5(180, 45) | 177.8, 205.7 | 8.26 | 948.3112 | $C_{44}H_{54}O_{22}N$ | -1.98 |
| 53 | 7.42 | 962.3→133.8(140, 55) | 133.8, 151.5 | 8.42 | 962.3274 | $C_{45}H_{56}O_{22}N$ | -1.46 |
| 54 | 7.66 | 962.3→175.6(140, 50) | 175.5, 193.5 | 8.66 | 962.3251 | $C_{45}H_{56}O_{22}N$ | -3.78 |
| 55 | 7.87 | 968.3→856.8(160, 30) | 203.5, 856.8 | 8.89 | 968.2695 | $C_{42}H_{50}O_{25}N$ | 2.83 |

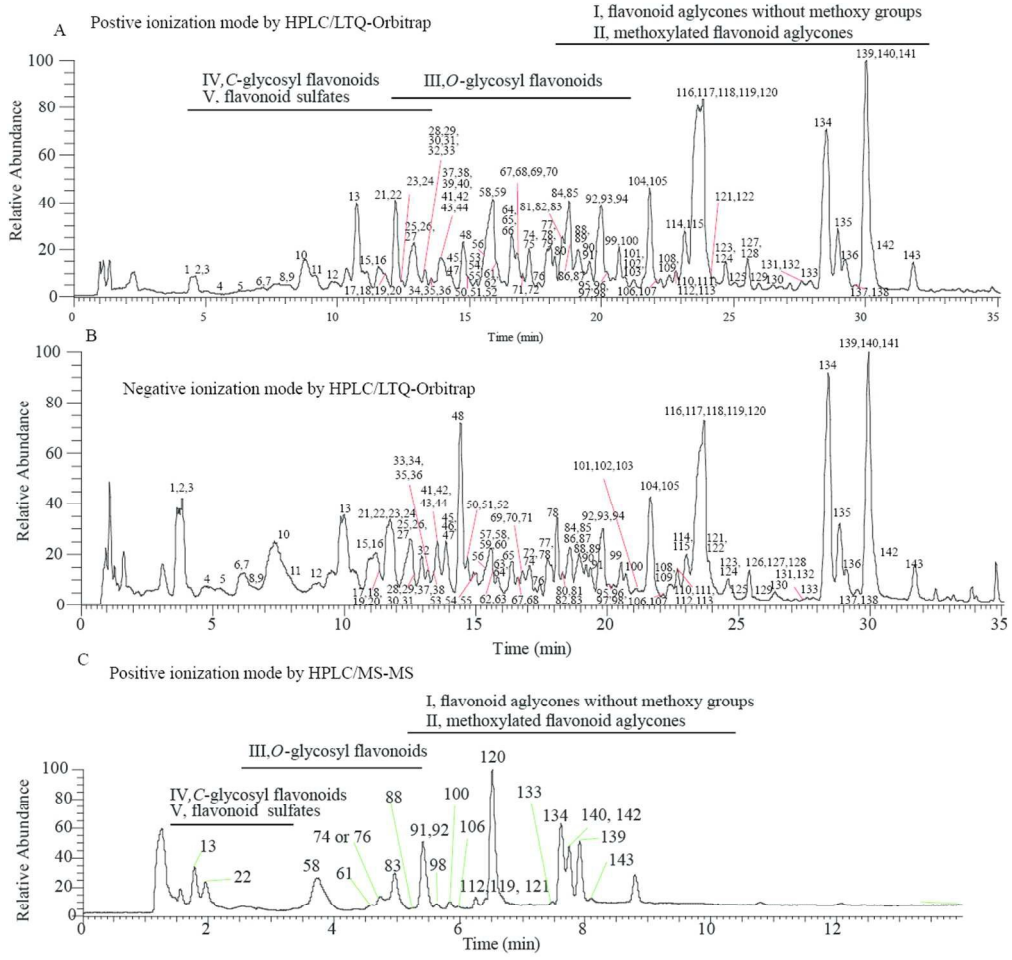


Fig.1

Total ion chromatograms of Scutellaria baicalensis extract obtained by HPLC/LTQ-Orbitrap-MS: (A) in positive ionization mode; (B) in negative ionization mode; (C) total ion chromatogramS of Scutellaria baicalensis extract obtained based on full mass scan monitoring by HPLC/MS-MS
203x203mm (150 x 150 DPI)

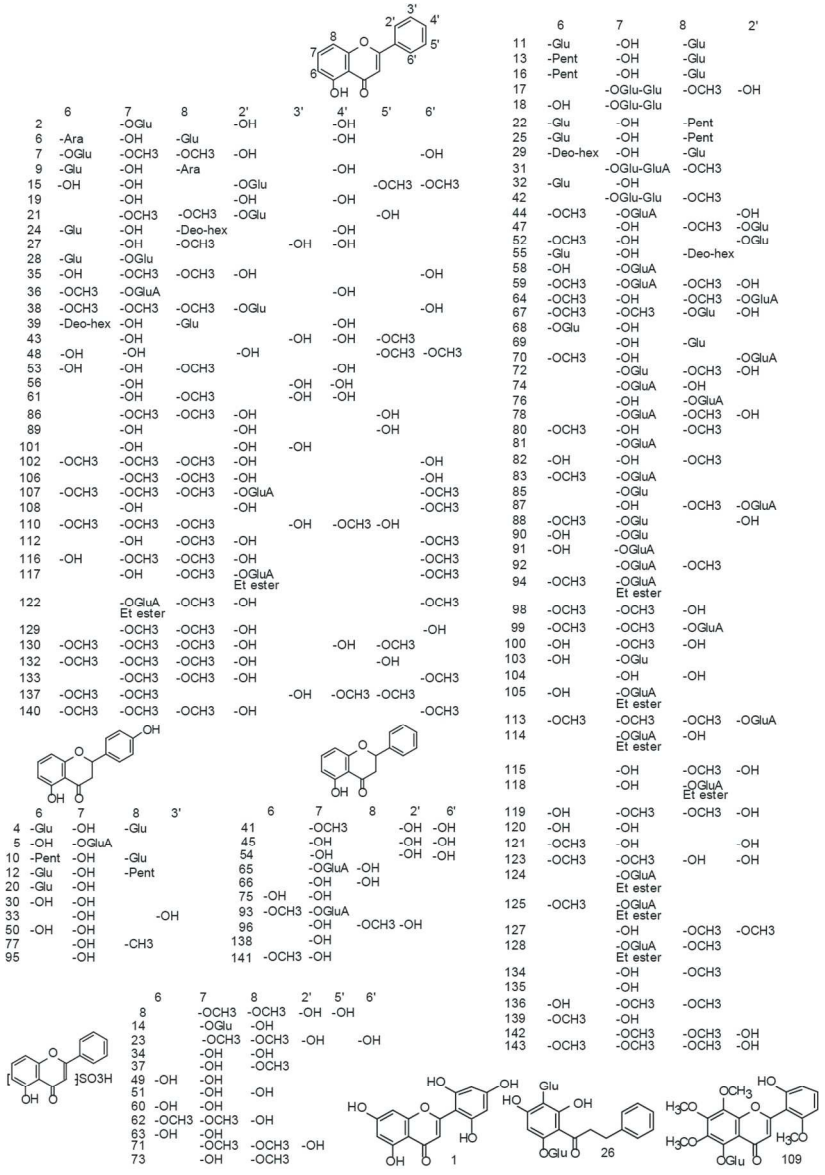


Fig. 2

209x309mm (150 x 150 DPI)

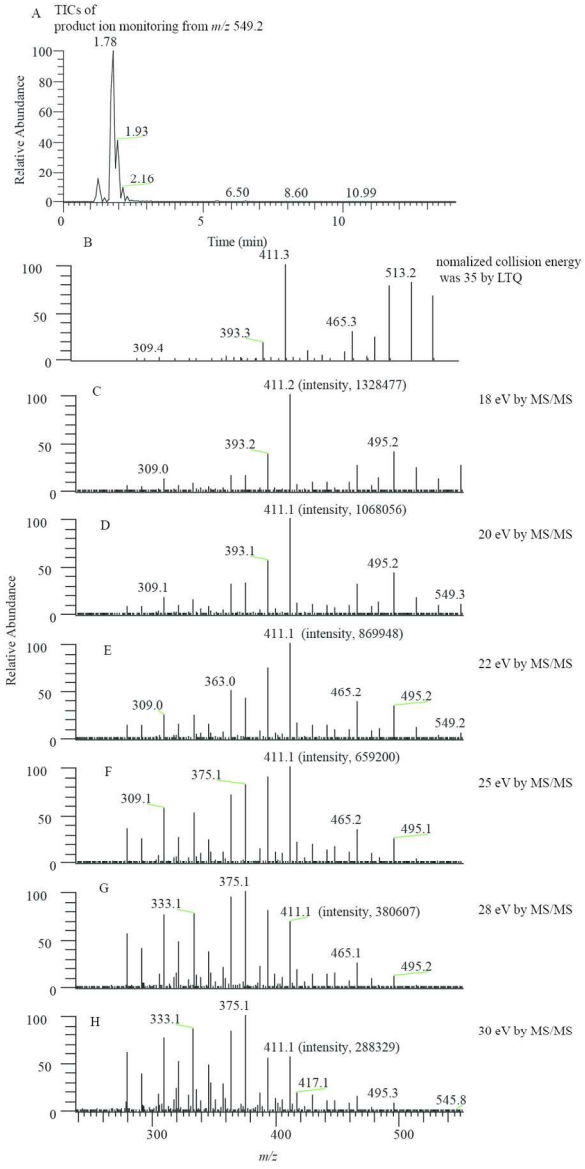


Fig. 3

182x379mm (150 x 150 DPI)

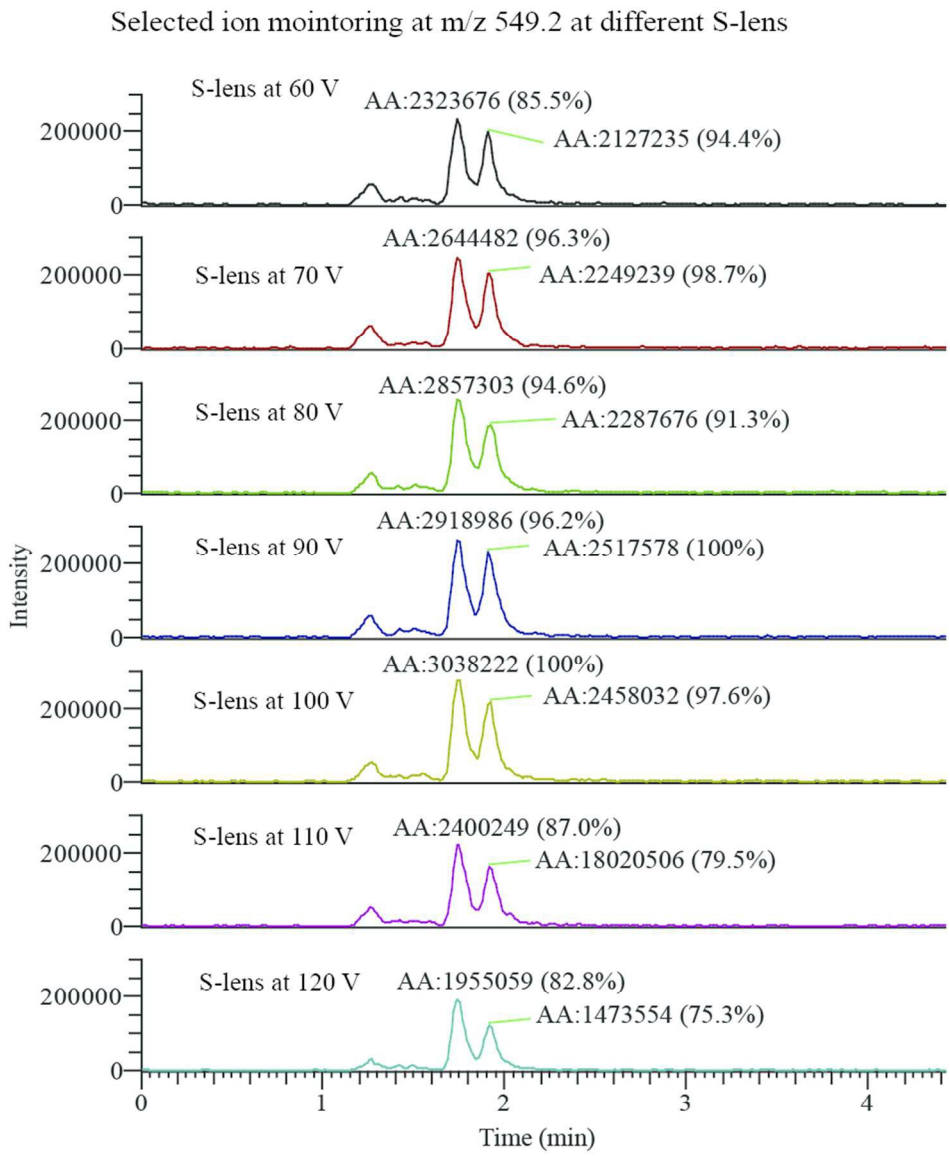


Fig. 4

159x203mm (150 x 150 DPI)

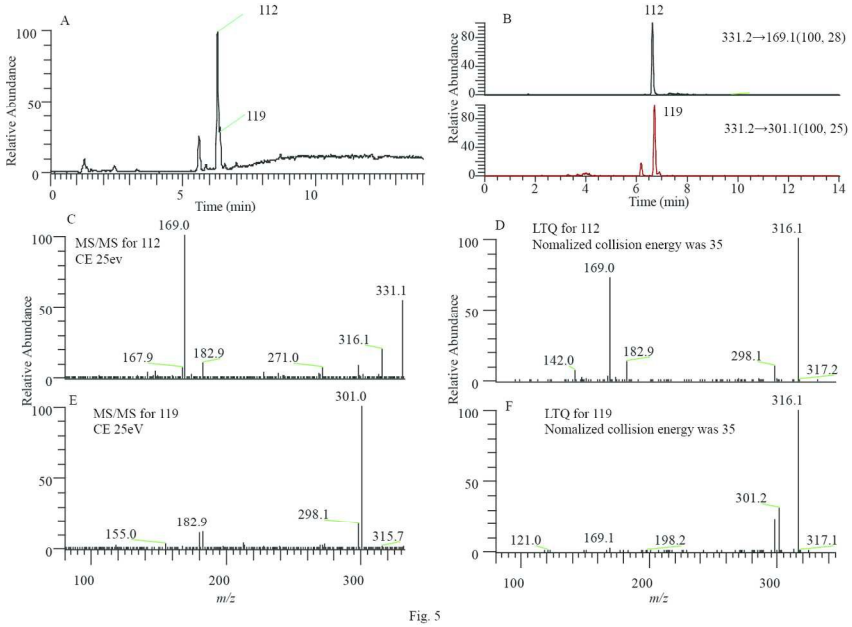


Fig. 5

313x194mm (150 x 150 DPI)

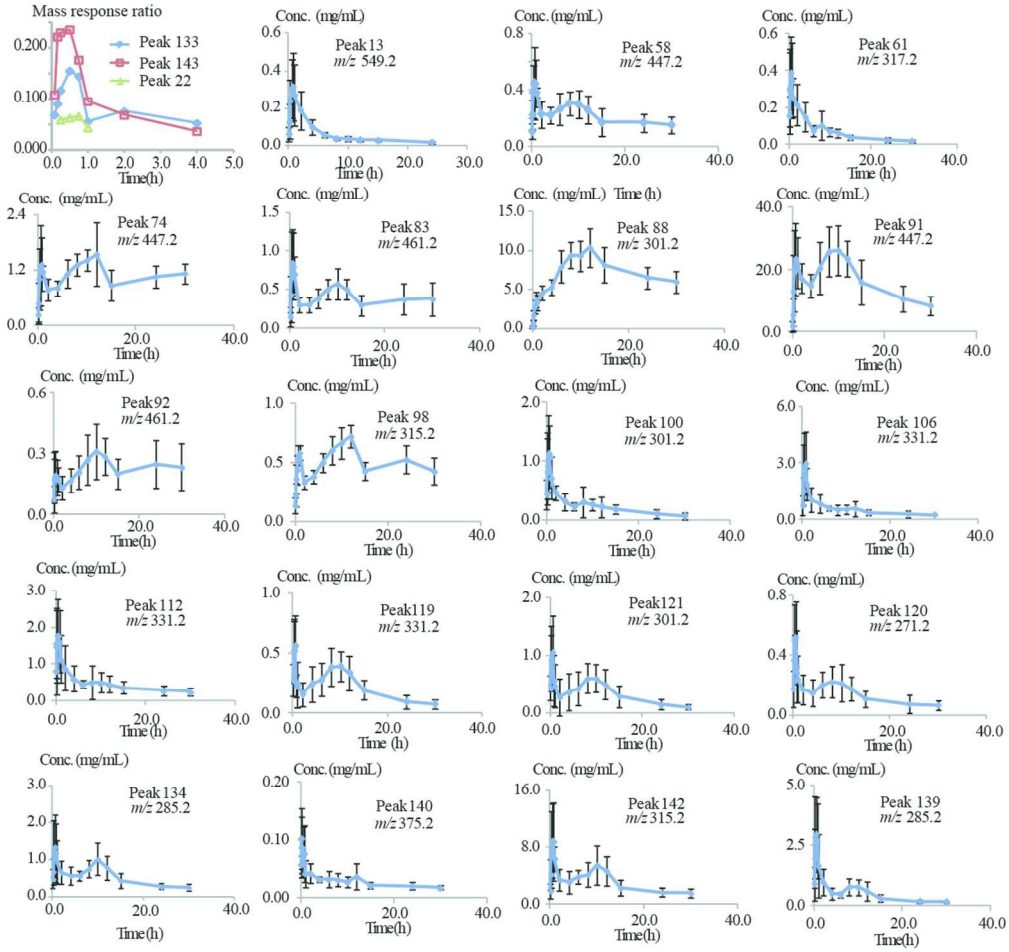


Fig. 6

216x211mm (150 x 150 DPI)

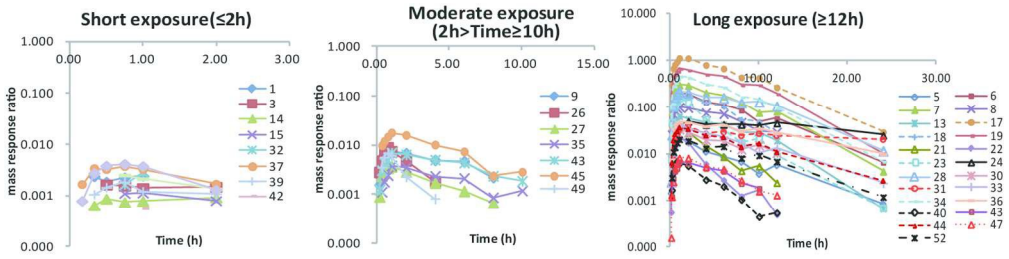


Fig. 7

299x91mm (150 x 150 DPI)